Electronic Supplementary Information

Long-term Spatiotemporal and Highly Specific Imaging of Plasma Membrane of Diverse Plant Cells Using a Near-Infrared AIE Probe

Jiaqi Zuo,[‡a] Engao Zhu,[‡b] Wenjing Yin,[b] Chuangye Yao,[a] Jiajia Liao,[a] Xinni Ping,[a] Yuqing Zhu,[a] Xuting Cai,[a] Yuchun Rao,[b] Hui Feng,[a] Kewei Zhang[b]* and Zhaosheng Qian[a]*

[a] Key Laboratory of the Ministry of Education for Advanced Catalysis Materials, College of Chemistry and Materials Science, Zhejiang Normal University, Jinhua 321004, China

[b] College of Life Sciences, Zhejiang Normal University, Jinhua 321004, China

Table of Contents

3. Supplementary Schemes and Figures

Scheme S1. Synthesis routes of APMem-1.

Figure S1. UV-visible spectrum of APMem-1 (20.0 μM) in DMSO.

Figure S2. Time-resolved PL decay curves of APMem-1 in dispersed in adamantane and APMem-1 in solid.

Figure S3. PL spectra of APMem-1 solution (100.0 μM) as the addition of SDBS from 0.0 to 300.0 μM.

Figure S4. PL spectra of APMem-1 (10.0 μM) in various solvents.

Figure S5. (A) UV-visible spectrum of APMem-1 (10.0 μM) in H_2O at various time points via a long-term irradiation (561nm 20mW); (B) The change of absorbance of the peak at 513 nm of APMem-1 (10.0 μM) in H_2O versus irradiation time by using the excitation source of 561 nm 20mW.

Figure S6. (A) PL spectra of APMem-1 (10.0 μM) in H_2O at various time points via a long-term irradiation (561nm 20mW); (B) The change of PL spectra of APMem-1 (10.0 μM) in H_2O at various time points via a long-term irradiation by using the excitation source of 561 nm 20mW.

Figure S7. (A) Change in PL intensity of the APMem-1 solution (20.0 μM) containing SDBS (20.0μM) versus pH values. λem = 644nm; (B) Change in mean PL intensity of a APMem-1 solution (20.0 μM) containing SDBS (20.0μM) versus pH values by using line charts. λem = 644nm; (C) The rate of change in PL intensity as pH changes of a APMem-1 solution (20.0 μM) containing SDBS (20.0μM) versus pH values by using line charts. λem = 644nm.

Figure S8. (a) Photographs of representative Arabidopsis thaliana seedlings incubated without (Mock) and with different concentrations of APMem-1 (10.0 μM to 50.0 μM) after 6 days. (b) Average root lengths of Arabidopsis thaliana seedlings incubated without (Mock) and with different concentrations of APMem-1 (10.0 μM to 50.0 μM) after 6 days.

Figure S9. Laser scanning confocal microscopy images of auto-fluorescence in Arabidopsis thaliana under 561 nm excitation. Scale bar = 50 μm.

Figure S10. Laser scanning confocal microscopy images in seedling roots of Arabidopsis thaliana stained with different amounts of APMem-1 for 5 min: (a, d) 5.0 μM; (b, e) 10.0 μM; (c, f) 20.0 μM.

Figure S11. Laser scanning confocal microscopy images in onion epidermal cells, which were first stained with APMem-1 (10.0 μM) for 5 min and then incubated in 0.3

g/mL sucrose solution for different times to achieve plasmolysis: (a, c) 0 min; (b, d) 20 min. Scale bar = 50 μm.

Figure S12. Laser scanning confocal microscopy images in onion epidermal cells, which were first stained with FM 1-43 and FM 4-64 (10.0 μM) for 5 min and then incubated in 0.3 g/mL sucrose solution for different times to achieve plasmolysis: (a, b) FM 1-43, Scale bar = 50 μm, 20 μm; (c, d) FM 4-64, Scale bar = 50 μm, 50 μm.

Figure S13. Laser scanning confocal microscopy images in onion epidermal cells, which were first stained with APMem-1 (10.0 μM) for 5 min and then incubated in sodium chloride solution for different concentration to achieve plasmolysis with 30min: (a) 0.5 mol/L NaCl, Scale bar = 50 μm; (b) The neonatal microvesicles in the process, Scale bar = 20 μm; (c) 1.0 mol/L NaCl, Scale bar = 50 μm.

Figure S14. Comparison of laser scanning confocal microscopy images of stained seedling roots of Arabidopsis thaliana (APMem-1, 10.0 μM, 5 min) treated with DMSO (b, d) and without DMSO (a, c). (a, c) Scale bar = 5 μm, (b, d) Scale bar = 10 μm.

Figure S15. (A) The changes of laser scanning confocal microscopy images in seedling roots of Arabidopsis thaliana stained with APMem-1 (10.0 μM) for 5 min versus irradiation time at 561 nm using the excitation source of the used microscope: (a) APMem-1 (0 min); (b) APMem-1 (10 min); (c) APMem-1 (20 min); (d) APMem-1 (30 min); (e) APMem-1 (40 min); (f) APMem-1 (50 min); (g) APMem-1 (60 min); (h) APMem-1 (70 min); (i) APMem-1 (80 min); (j) APMem-1 (90 min). Scale bar = 10 μm. (B) The change of PL intensity of APMem-1 inserted inside the cell membranes versus irradiation time at 561 nm using the excitation source of the used microscope.

Figure S16. Laser scanning confocal microscopy images in seedling roots of Arabidopsis thaliana stained with APMem-1 (10.0 μM probes incubated for 5 min) at various time points: (a, g) APMem-1 (0.5 h); (b, h) APMem-1 (1 h); (c, i) APMem-1 (2 h); (d, j) APMem-1 (3 h); (e, k) APMem-1 (4 h); (f, l) APMem-1 (5 h); (m, r) APMem-1 (6 h); (n, s) APMem-1 (7 h); (o, t) APMem-1 (8 h); (p, u) APMem-1 (9 h); (q, v) APMem-1 (10 h). Scale bar = 10 μm.

Figure S17. Laser scanning confocal microscopy images of seedling roots of Arabidopsis thaliana stained with (A) FM 1-43 (B) FM 4-64 (10.0 μM probes incubated for 5 min) at various time points. (a, b, e, f, g, h) Scale bar= 20 μm; (c, d, i, j, k, l) Scale bar= 10 μm.

Figure S18. The values of f_{Signal} /$f_{Background}$ during 1 – 10 h imaging time.

Figure S19. High-resolution image analyses of imaging performance for seedling roots of Arabidopsis thaliana stained with APMem-1 in imaging completeness and

imaging specificity. $S_{imaging}$ and $S_{Background}$ represent the ratios of signal area and background area to the whole area.

Figure S20. Laser scanning confocal microscopy images in onion epidermal cells, which were first stained with APMem-1 (10.0 μM) for 5 min and then incubated with different concentrations of NaCl solution at various time points (A) 0.1 mol/L NaCl, Scale bar = 50 μm; 0.2 mol/L NaCl, Scale bar = 50 μm; (B) 0.5 mol/L NaCl, Scale bar = 50 μm (n: 20 μm); 1.0 mol/L NaCl; Scale bar = 50 μm.

Figure S21. Laser scanning confocal microscopy images in onion epidermal cells, which were first stained with FM 4-64 (10.0 μM) for 5 min and then incubated in 0.5mol/L NaCl solution at various time points to achieve plasmolysis; Scale bar = 50 μm.

4. Spectra of Compounds

Figure S22 ^{1}H NMR spectra of 4-(hexyloxy)-N-phenylaniline in $CDCl_3$

Figure S23 ^{13}C NMR spectra of 4-(hexyloxy)-N-phenylaniline in $CDCl_3$

Figure S24 ^{1}H NMR spectra of 4-((4-(hexyloxy)phenyl)(phenyl)amino)benzaldehyde in $CDCl_3$

Figure S25 ^{13}C NMR spectra of 4-((4-(hexyloxy)phenyl)(phenyl)amino)benzaldehyde in $CDCl_3$

Figure S26 ^{1}H NMR spectra of 3-(4-((4-(hexyloxy)phenyl)(phenyl)amino)phenyl)-2-(pyridin-4-yl)acrylonitrile in $CDCl_3$

Figure S27 ^{13}C NMR spectra of 3-(4-((4-(hexyloxy)phenyl)(phenyl)amino)phenyl)-2-(pyridin-4-yl)acrylonitrile in $CDCl_3$

Figure S28 ^{1}H NMR spectra of 1-(3-bromopropyl)-4-(1-cyano-2-(4-((4-(hexyloxy) phenyl)(phenyl)amino)phenyl)vinyl)pyridin-1-ium in $CDCl_3$

Figure S29 ^{13}C NMR spectra of 1-(3-bromopropyl)-4-(1-cyano-2-(4-((4-(hexyloxy)phenyl)(phenyl)amino)phenyl)vinyl)pyridin-1-ium in $CDCl_3$

Figure S30 ^{1}H NMR spectra of (Z)-1-(3-(4-(1-cyano-2-(4-((4-(hexyloxy)phenyl)(phenyl)amino)phenyl)vinyl)pyridin-1-ium-1-yl)propyl)-1,4-diazabicyclo [2.2.2]octan-1-ium in $CDCl_3$

Figure S31 ^{13}C NMR spectra of spectra of (Z)-1-(3-(4-(1-cyano-2-(4-((4-(hexyloxy)phenyl)(phenyl)amino)phenyl)vinyl)pyridin-1-ium-1-yl)propyl)-1,4-diazabicyclo [2.2.2]octan-1-ium in CD_3OD

Figure S32 High-resolution mass spectrum of 4-(hexyloxy)-N-phenylaniline

Figure S33 High-resolution mass spectrum of 4-((4-(hexyloxy)phenyl)(phenyl)amino) benzaldehyde

Figure S34 High-resolution mass spectrum of (Z)-3-(4-((4-(hexyloxy)phenyl) (phenyl)

1. Experimental Section

Synthesis of 4-(hexyloxy)-N-phenylaniline (2). Cesium carbonate (7.82 g, 24 mmol) was added to 30 mL of dry DMF in a 50 mL two necked flask, and then 4-hydroxydiphenylamine (1.85 g, 10 mmol) and 1-bromohexane (1.98 g, 12 mmol) were added under N_2 atmosphere respectively. The system was stirred at 95℃ for 48 h. The solution finally turned into brown-black. After cooling to room temperature, the mixture was poured into water and then extracted with ethyl acetate. The organic layer was washed with water 3 times (3×50 mL) and dried by anhydrous Na_2SO_4. All solvents were removed from the system by rotary evaporation. The crude product was purified by column chromatography (EA:PE=1:20) to give 4-(hexyloxy)-N-phenylaniline as a light pink solid (2.42 g, 90%). Molecular formula: $C_{18}H_{23}NO$. ^1H NMR (600 MHz, $CDCl_3$), δ (ppm): 7.20 (t, J = 7.8 Hz, 2H), 7.05 (t, 2H), 6.90 (t, J = 7.3 Hz, 2H), 6.87 – 6.79 (m, 3H), 5.50 (s, 1H), 3.93 (t, J = 6.4 Hz, 2H), 1.77 (m, 2H), 1.48 – 1.43 (m, 2H), 1.36 – 1.31 (m, 4H), 0.91 (t, 3H). ^{13}C NMR (151 MHz, $CDCl_3$), δ (ppm): 129.56, 122.55, 119.79, 119.78, 115.90, 115.88, 115.62, 115.60, 68.71, 31.90, 29.62, 26.04, 22.91, 14.33. ESI HRMS (m/z): calcd. for $C_{18}H_{23}NO$ $[M+H]^+$: 270.1852, found: 270.1856.

Synthesis of 4-((4-(hexyloxy)phenyl)(phenyl)amino)benzaldehyde (3). In the N_2 atmosphere, cesium carbonate (3.9 g, 12 mmol), 4-(hexyloxy)-N-phenylaniline (0.538 g, 2 mmol), 4-bromobenzaldehyde (1.1 g, 6 mmol), $Pd(OAc)_2$ (0.05 g) and $P(t\text{-}Bu)_3$ (1 mL) were added in sequence to a 250 mL three necked flask containing 100 mL toluene. The resulting mixture was stirred at 110°C for 48 h. After cooling to room temperature, the mixture was poured into water and then extracted with ethyl acetate. The organic layer was washed with water 3 times (3×50 mL) and dried by anhydrous Na_2SO_4. All solvents were removed from the system by rotary evaporation. The crude product was purified by column chromatography (EA:PE=1:200) to give a yellow-green and gelatinous product (0.71 g, 95%). Molecular formula: $C_{25}H_{27}NO_2$. ^1H NMR (600 MHz, $CDCl_3$), δ (ppm): 9.78 (s, 1H), 7.67 – 7.63 (m, 2H), 7.35 – 7.30 (m, 2H), 7.19 – 7.09 (m, 5H), 6.94 (d, J = 8.8 Hz, 2H), 6.91 – 6.87 (m, 2H), 3.95 (t, J = 6.5 Hz, 2H), 1.82 – 1.75 (m, 2H), 1.49 – 1.44 (m, 2H), 1.37 – 1.33 (m, 4H), 0.94 –0.88 (m, 3H). ^{13}C NMR (151 MHz, $CDCl_3$), δ (ppm): δ 190.62, 157.39, 153.96, 146.42, 138.83, 131.61, 129.89, 128.71, 128.64, 126.09, 125.06, 118.35, 115.92, 68.55, 31.86, 29.53, 26.02, 22.89, 14.32. ESI HRMS (m/z): calcd. for $C_{25}H_{27}NO_2$ $[M+H]^+$: 374.2115, found: 374.2100.

Synthesis of (Z)-3-(4-((4-(hexyloxy)phenyl)(phenyl)amino)phenyl)-2-(pyridin-4-yl)acrylonitrile (4). 4-((4-(hexyloxy)phenyl)(phenyl)amino)benzaldehyde (0.5 g, 1.34 mmol) was dissolved in methanol and stirred at room temperature. To this solution, 4-pyridine acetonitrile (0.316 g, 2 mmol) and sodium methoxide (0.145 g, 2.66 mmol) were added and the reaction mixture was stirred at 80℃ for 5 h. After cooling to room temperature, the mixture was extracted with ethyl acetate. The organic layer was washed with water 3 times (3×50 mL) and dried by anhydrous Na_2SO_4. All solvents were removed from the system by rotary evaporation. The crude product was purified by column chromatography (EA:PE=1:2) to give a brownish and gelatinous product (0.60 g, 95%). Molecular formula: $C_{32}H_{31}N_3O$.^1H NMR (400 MHz, $CDCl_3$), δ (ppm): 8.64 (s, 2H), 7.80 (d, J = 8.8 Hz, 2H), 7.58 (s, 1H), 7.52 (d, J = 5.2 Hz, 2H), 7.32 (t, J = 7.9 Hz, 2H), 7.17 (d, J = 8.0 Hz, 2H), 7.13 (t, J = 7.9 Hz, 3H), 6.97 (d, J = 8.9 Hz, 2H), 6.89 (d, J = 8.9 Hz, 2H), 3.96 (t, J = 6.5 Hz, 2H), 1.83 – 1.77 (m, 2H), 1.50 – 1.45 (m, 2H), 1.37 – 1.33 (m, 4H), 0.92 (t, J = 6.9 Hz, 3H). ^{13}C NMR (150 MHz, $CDCl_3$), δ (ppm): 157.04, 151.38, 150.41, 146.20, 144.39, 142.65, 138.61, 131.53, 129.57, 128.30, 125.50, 124.57, 124.31, 119.52, 118.85, 117.95, 115.65, 103.68, 68.29, 31.59, 29.26, 25.75, 22.61, 14.20. ESI HRMS (m/z): calcd. for $C_{32}H_{31}N_3O$ $[M+H]^+$: 474.2540, found: 474.2524.

Synthesis of (Z)-1-(3-bromopropyl)-4-(1-cyano-2-(4-((4-(hexyloxy)phenyl)(phenyl)amino)-phenyl)vinyl)pyridin-1-ium (5). (Z)-3-(4-((4-(hexyloxy)phenyl)(phenyl)amino)phenyl)-2-(pyridin-4-yl)acrylonitrile (0.2 g 0.42 mmol) was dissolved in dry acetonitrile and stirred at room temperature. Under N_2 atmosphere, 1,3-dibromopropane (1.28 g 6.3 mmol) were added and the reaction mixture was stirred at 110℃ for 48 h. After cooling to room temperature, the solvent was removed by evaporation under reduced pressure. The residue was washed with petroleum ether at least

three times to get rid of most of unreacted 1,3-dibromopropane under ultrasonic condition. The residual solvent on their surface were evaporated under reduced pressure to give a dark purple powder (0.21 g, 75%). Molecular formula: $C_{35}H_{37}Br_2N_3O$. ^{1}H NMR (400 MHz, $CDCl_3$), δ (ppm): 9.17 (s, 2H), 8.46 (s, 1H), 8.35 (s, 2H), 8.07 (d, J = 8.6 Hz, 2H), 7.36 (t, J = 7.7 Hz, 2H), 7.19 (t, J = 7.7 Hz, 3H), 7.12 (d, J = 8.4 Hz, 2H), 6.89 (t, 4H), 5.01 (s, 2H), 3.96 (t, J = 6.4 Hz, 2H), 3.51 (s, 2H), 2.67 (s, 2H), 1.82 – 1.77 (m, 2H), 1.49 – 1.44 (m, 2H), 1.37 – 1.33 (m, 4H), 0.91 (t, J = 7.0 Hz, 3H). ^{13}C NMR (151 MHz, $CDCl_3$), δ (ppm): 157.68, 153.72, 152.21, 151.45, 145.04, 144.15, 137.42, 134.57, 129.83, 128.49, 126.37, 125.95, 123.37, 122.46, 117.72, 117.23, 115.76, 97.31, 68.33, 58.78, 33.68, 31.58, 29.21, 29.06, 25.73, 22.62, 14.07. ESI HRMS (m/z): calcd. for $C_{35}H_{37}Br_2N_3O$ $[M\text{-}Br]^+$: 594.2115, found: 594.2144.

Synthesis of APMem-1. (Z)-1-(3-bromopropyl)-4-(1-cyano-2-(4-((4-(hexyloxy)phenyl)(phenyl)amino)phenyl)-vinyl)pyridin-1-ium and 1,4-diazabicyclo[2.2.2]octane were heated to reflux atstirred at 85℃ under N_2 atmosphere in a 150 mL two necked flask for 20 h. Dark purple precipitates formed during the reaction. After cooling down, the solvent was removed by evaporation under reduced pressure. The crude product was washed with a mixed solution of petroleum ether and acetone (petroleum ether: acetone =5:1) at least three times under ultrasonic condition. The residual solvent on their surface were evaporated under reduced pressure to give a dark purple solid. Yield: 70%. Molecular formula: $C_{41}H_{49}Br_2N_5O$. ^{1}H NMR (400 MHz, $CDCl_3$), δ (ppm): 9.15 (s, 2H), 8.32 (d, J = 13.3 Hz, 3H), 8.05 (d, J = 8.6 Hz, 2H), 7.36 (t, J = 7.5 Hz, 2H), 7.21 (d, J = 8.4 Hz, 2H), 7.12 (d, J = 8.8 Hz, 2H), 6.91 (d, J = 8.6 Hz, 5H), 4.97 (s, 2H), 3.96 (t, J = 6.4 Hz, 2H), 3.49 (d, J = 5.0 Hz, 2H), 2.69 (s, 2H), 1.81 – 1.78 (m, 12H), 1.36 – 1.34 (m, 4H), 1.28 – 1.25 (m, 4H), 0.89 – 0.87 (m, 3H). ^{13}C NMR (150 MHz, CD_3OD), δ (ppm): 141.09, 132.88, 129.69, 129.45, 128.26, 127.25, 127.16, 125.90, 125.64, 124.89, 121.48, 118.50, 115.52, 67.98, 60.39, 55.16, 52.72, 52.40, 51.19, 44.66, 44.49, 31.37, 29.35, 28.99, 28.61, 25.47, 23.49, 22.30, 13.00. ESI HRMS (m/z): calcd. for $C_{41}H_{49}Br_2N_5O$ $[M\text{-}2Br]^{2+}$: 313.6963, found: 313.6957.

2. Experimental Procedures

2.1 Characterization of UV-Visible and Fluorescence Properties of All Samples

UV−vis absorption spectra were recorded using an Agilent Cary 5000 UV-Vis-NIR spectrophotometer. Steady PL spectra of all samples were performed on an Edinburgh Instruments model FLS980 fluorescence spectrophotometer equipped with a xenon arc lamp using a front face sample holder. Time-resolved fluorescence measurements were conducted with EPL-series lasers.

2.2 Fluorescence Turn-on Assay of Probe

A solution of sodium dodecylbenzene sulfonate (SDBS) with a fixed concentration (200 μM) in triple-distilled water was first prepared, and then different amounts of probe in the range of 0.0 – 12 μM were separately added into the preceding probe solutions. The fluorescence spectra of the resulting mixtures were recorded at the excitation of 483 nm using a xenon arc lamp. A series of mixed solutions of glycerol and DMSO were prepared (glycerol volume fraction varied from 0% to 99%). Fluorescence intensity of 100 μM probes at around 649 nm with different glycerin/DMSO volume fractions (λ_{ex} = 395nm) were measured and recorded.

2.3 Effect of pH on Probe

A series of 0.2 M PBS buffers with different pH values (pH = 5.7, 6.0, 6.5, 7.0, 7.5 and 8.0) were prepared, then probes and sodium dodecylbenzene sulfonate were added to them at concentrations of 20 μM. The resulting solutions were monitored using fluorescence spectrometer at 644 nm emission. All the detections were repeated at least three times.

2.4 Toxicity Test of APMem-1 towards *Arabidopsis Thaliana*

The wild-type (Col-0) seeds of *Arabidopsis thaliana* were surface sterilized and imbibed for 3 days at 4°C in dark and then sown onto 0.5×Murashige & Skoog (MS) 1.5% (w/v) agar plates. Seedlings were vertically grown on plates in a climate-controlled growth room (22/20°C day/night temperature, 16/8 h photoperiod, and 80 $\mu mol \cdot s^{-1} \cdot m^{-2}$ light intensity). The first group of *Arabidopsis thaliana* was grown under the preceding normal conditions. The other five groups of *Arabidopsis thaliana* were grown on 0.5×Murashige & Skoog (MS) 1.5% (w/v) agar plates containing additional APMem-1 (10 μM, 20 μM, 30 μM, 40 μM and 50 μM). The resulting phenotype of two groups was recorded using a camera.

2.5 Cell Membrane Imaging of Root Cells of *Arabidopsis Thaliana*

The wild-type (Col-0) seeds of *Arabidopsis thaliana* were surface sterilized and imbibed for 3 days at 4°C in dark and then sown onto 0.5×Murashige & Skoog (MS) 1.5% (w/v) agar plates. Seedlings were vertically grown on plates in a climate-controlled growth room (22/20°C day/night temperature, 16/8 h photoperiod, and 80 $\mu mol \cdot s^{-1} \cdot m^{-2}$ light intensity). Five-day-old seedlings with healthy roots were used in this study unless otherwise specified. 1/2 MS culture medium and stock solutions of the probes in DMSO (20.0 mM) were prepared. After that, 1 μL stock solution of APMem-1 was added to 2 mL 1/2 MS culture medium to get a final staining dye concentration at 10.0 μM, respectively. The *Arabidopsis thaliana* seedlings were incubated with the probe for 5 min at 22°C. Fluorescence imaging experiment was performed on a Leica TCS SP5 model confocal laser scanning microscope (Germany) with an excitation at 561 nm.

During the photostability experiment, the fluorescence of APMem-1 after inserted into the plasma membrane was directly recorded in a normal mode. The root cells were respectively incubated with APMem-1 (10.0 μM, 5 min), and then continuously irradiated at 561 nm in the range of 0 – 15 min. During the intervals, their fluorescence signals were separately recorded under the respective optimum acquisition conditions in a normal mode. The change in fluorescence of APMem-1 was observed after different irradiation times.

2.6 Cell Membrane Imaging of Root and Leaf Cells of Tobacco

The seeds of tobacco were surface sterilized and then sown onto 0.5×Murashige & Skoog (MS) 1.5% (w/v) agar plates. Seedlings were vertically grown on plates in a climate-controlled growth room (28°C temperature, 14/10 h photoperiod, and 80 $\mu mol \cdot s^{-1} \cdot m^{-2}$ light intensity). Four-day-old seedlings with healthy roots were used in this study unless otherwise specified. The operation method of probe-specific imaging experiment was the same as that of *Arabidopsis thaliana*.

2.7 Cell Membrane Imaging of Root Cells of Rice

The wild-type seeds of rice were shelled and surface sterilized, then sown onto 0.5×Murashige & Skoog (MS) 1.5% (w/v) agar plates. Seedlings were vertically grown on plates in a climate-controlled growth room (28°C temperature, 14/10 h photoperiod, and 80 $\mu mol \cdot s^{-1} \cdot m^{-2}$ light intensity). Three-day-old seedlings with healthy roots were used in this study unless otherwise specified. The operation method of probe-specific imaging experiment was the same as that of *Arabidopsis thaliana*.

2.8 Plasmolysis of Onion Epidermal Cells

Use tweezers to take off a few pieces of onion endepidermis. These endepidermis were stained with APMem-1 (10.0 μM) for 5 min, then taken to sucrose solution (0.3 g/mL). One piece of them was taken out every 10 min for observation, and the targeting of APMem-1 probe to cell membrane were studied through the process of plasmolysis.

2.9 DMSO-induced Plasma Membrane Damage Experiment

The wild-type (Col-0) seeds of Arabidopsis thaliana were surface sterilized and imbibed for 3 days at 4°C in dark and then sown onto 0.5×Murashige & Skoog (MS) 1.5% (w/v) agar plates. Seedlings were vertically grown on plates in a climate-controlled growth room (22/20℃ day/night temperature, 16/8 h photoperiod, and 80 $\mu mol \cdot s^{-1} \cdot m^{-2}$ light intensity).

The plasma membranes of root cells of Arabidopsis thaliana were incubated with APMem-1 for 5 min at 22°C. Fluorescence imaging experiment was performed on a Leica TCS SP5 model confocal laser scanning microscope (Germany) with an excitation at 561 nm. The control group was treated by the same method as above except that the Arabidopsis seedlings were placed in 50 % DMSO aqueous solution for one second after staining. After the treatment of DMSO, seedling root of Arabidopsis thaliana were placed on slides and imaged on a Leica TCS SP5 model confocal laser scanning microscope (Germany) with an excitation at 561 nm.

2.10 The Statistical Data Process Details of Quantitative Analysis

The statistically quantitative data including brightness contrast, imaging integrity and signal ratio. As for brightness, we used "$f_{Signal}/f_{Background}$" to represent and it can be quantified by the software "ImageJ". We imported the merged image into the software and separated the channels, selected the dark field channel and clicked "Threshold" to calculate the Mean (Mean gray value). "Cell integrity" was evaluated by the ratio of the number of intact cells via signal-imaging to the total number of cells in the imaging field. The value for "$S_{Imaging}$" from high-resolution pixel analysis was realized with "Adobe Photoshop CS6" software. After importing the image, we used the "Color Picker" in the "Color Range" option to select the "signal region" with red. After finishing the selection, the "Measurement Log" operation can be performed, and the obtained "Area" corresponds to the "$S_{Imaging}$". Repeating the same operation, the area of "non-signal region" can be gained by reverse selection.

3. Supplementary Schemes and Figures

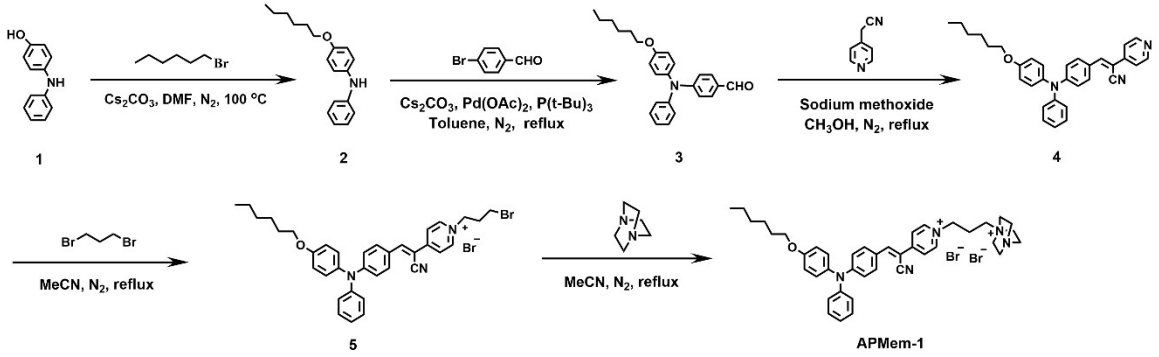

Scheme S1. Synthesis routes of APMem-1.

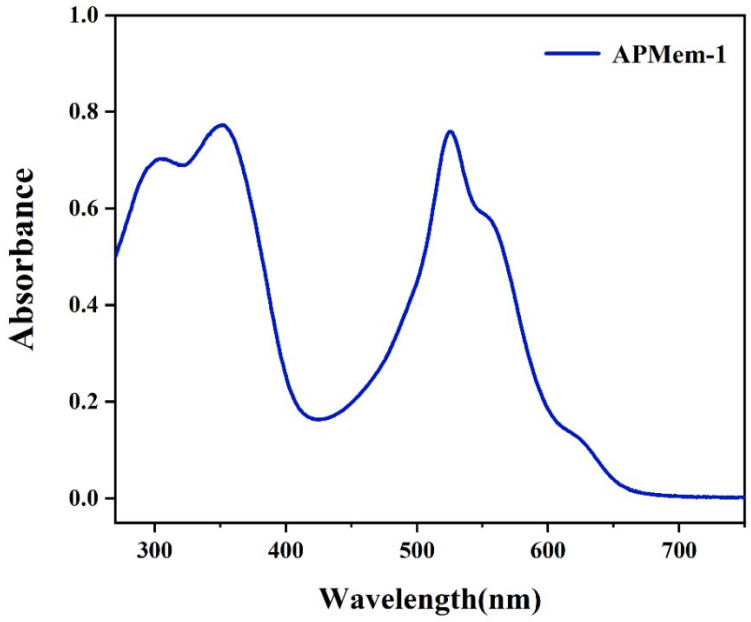

Figure S1. UV-visible spectrum of APMem-1 (20.0 μM) in DMSO.

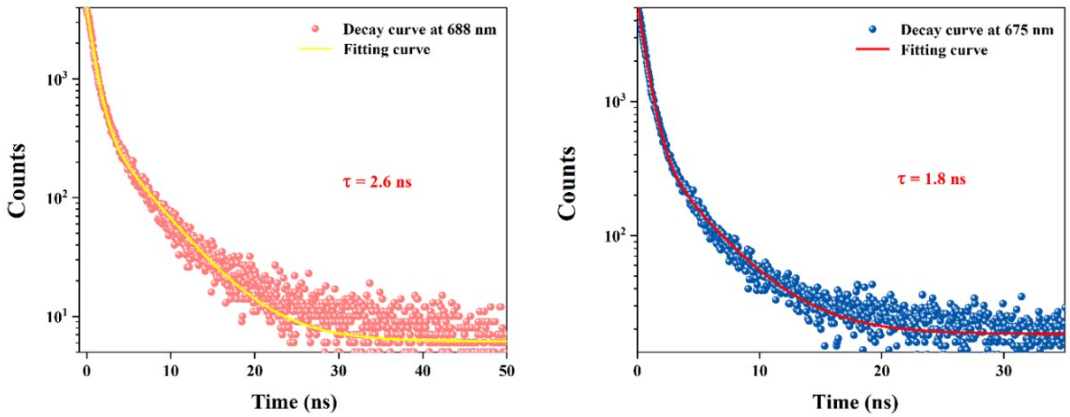

Figure S2. Time-resolved PL decay curves of APMem-1 in dispersed in adamantane and APMem-1 in solid.

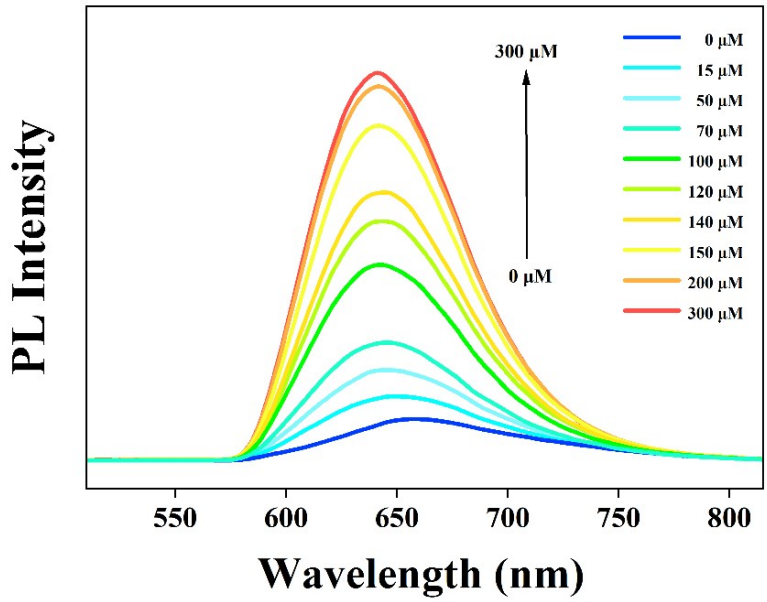

Figure S3. PL spectra of APMem-1 solution (100.0 μM) as the addition of SDBS from 0.0 to 300.0 μM.

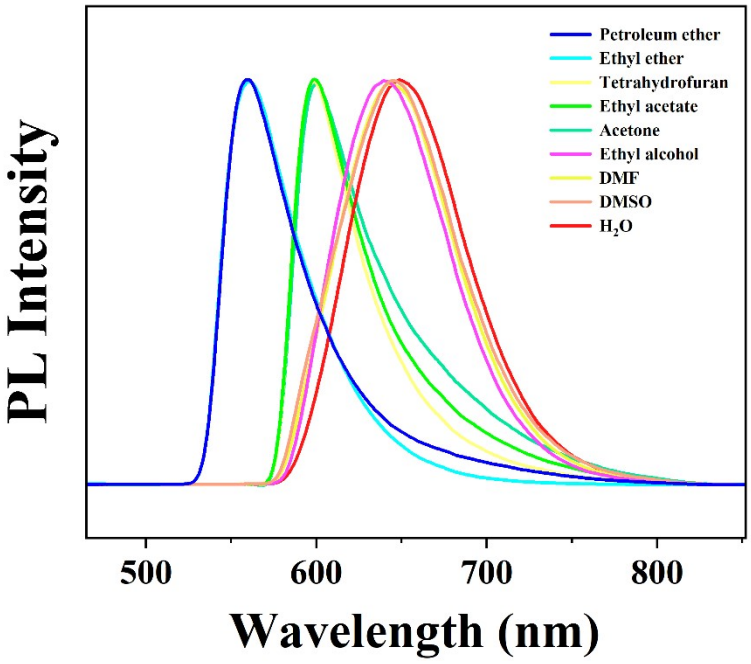

Figure S4. PL spectra of APMem-1 (10.0 μM) in various solvents.

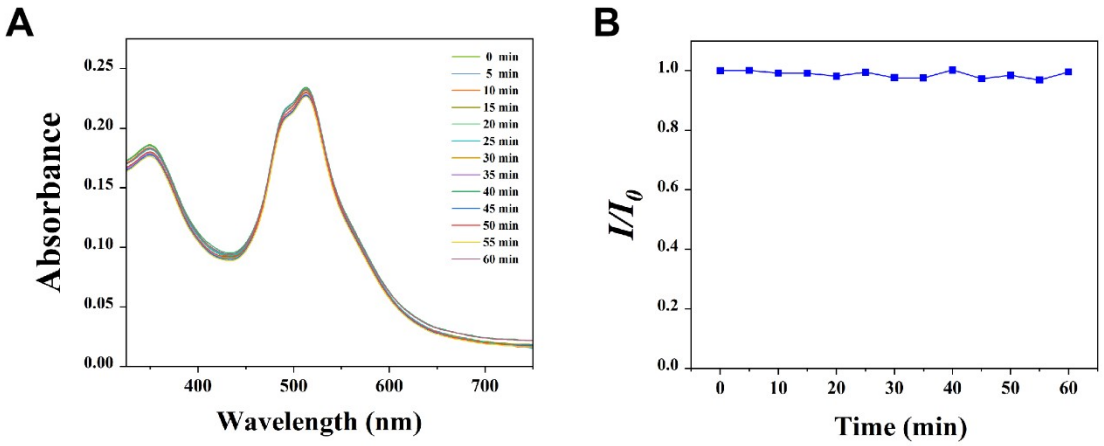

Figure S5. (A) UV-visible spectrum of APMem-1 (10.0 μM) in H_2O at various time points via a long-term irradiation (561nm 20mW); (B) The change of absorbance of the peak at 513 nm of APMem-1 (10.0 μM) in H_2O versus irradiation time by using the excitation source of 561 nm 20mW.

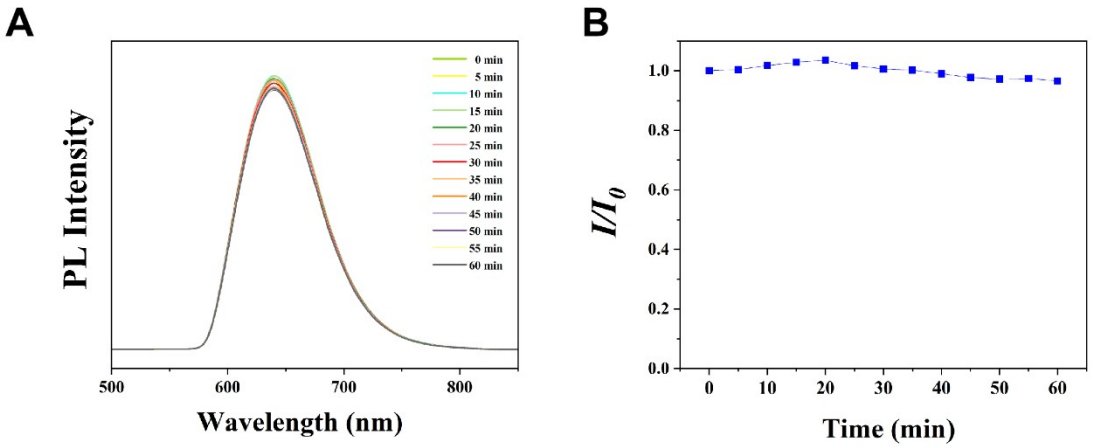

Figure S6. (A) PL spectra of APMem-1 (10.0 μM) in H_2O at various time points via a long-term irradiation (561nm 20mW); (B) The change of PL spectra of APMem-1 (10.0 μM) in H_2O at various time points via a long-term irradiation by using the excitation source of 561 nm 20mW.

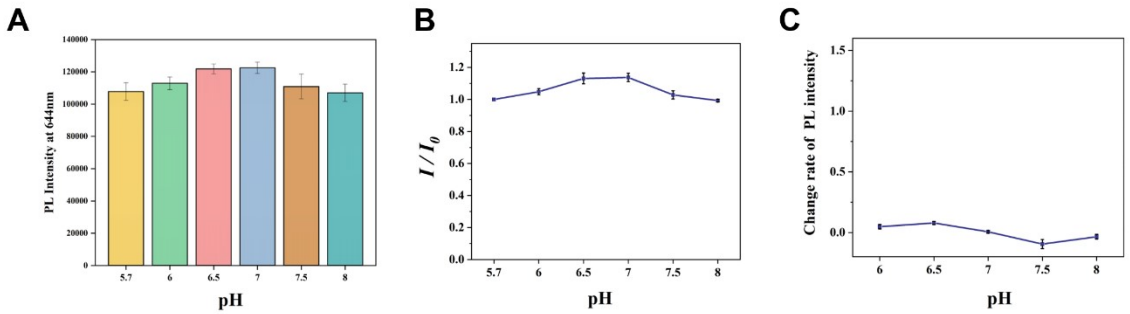

Figure S7. (A) Change in PL intensity of the APMem-1 solution (20.0 μM) containing SDBS (20.0 μM) versus pH values. λ_{em} = 644nm; (B) Change in mean PL intensity of a APMem-1 solution (20.0 μM) containing SDBS (20.0 μM) versus pH values by using line charts. λ_{em} = 644nm; (C) The rate of change in PL intensity as pH changes of a APMem-1 solution (20.0 μM) containing SDBS (20.0 μM) versus pH values by using line charts. λ_{em} = 644nm.

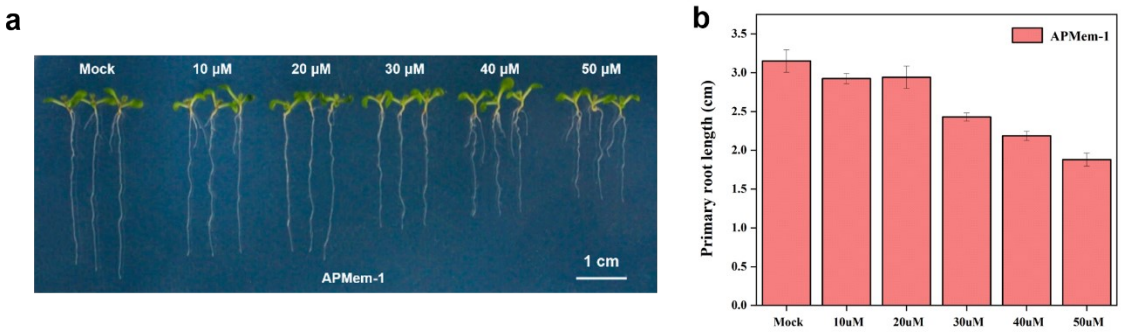

Figure S8. (a) Photographs of representative *Arabidopsis thaliana* seedlings incubated without (Mock) and with different concentrations of APMem-1 (10.0 μM to 50.0 μM) after 6 days. (b) Average root lengths of *Arabidopsis thaliana* seedlings incubated without (Mock) and with different concentrations of APMem-1 (10.0 μM to 50.0 μM) after 6 days.

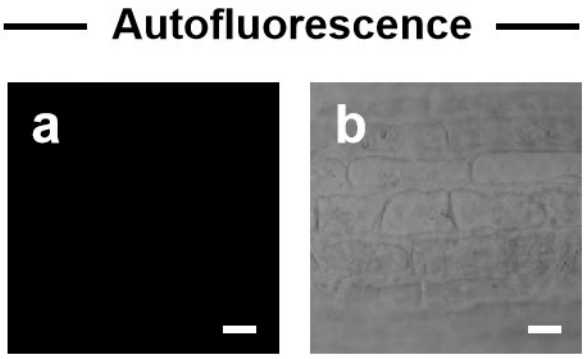

Figure S9. Laser scanning confocal microscopy images of auto-fluorescence in Arabidopsis thaliana under 561 nm excitation. Scale bar = 50 μm.

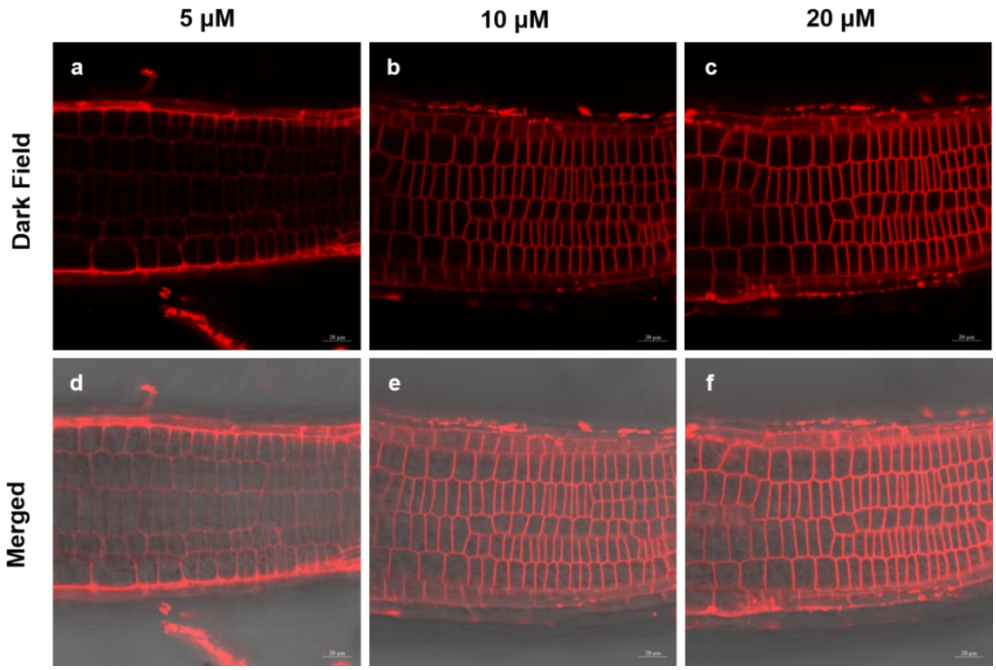

Figure S10. Laser scanning confocal microscopy images in seedling roots of *Arabidopsis thaliana* stained with different amounts of APMem-1 for 5 min: (a, d) 5.0 μM; (b, e) 10.0 μM; (c, f) 20.0 μM.

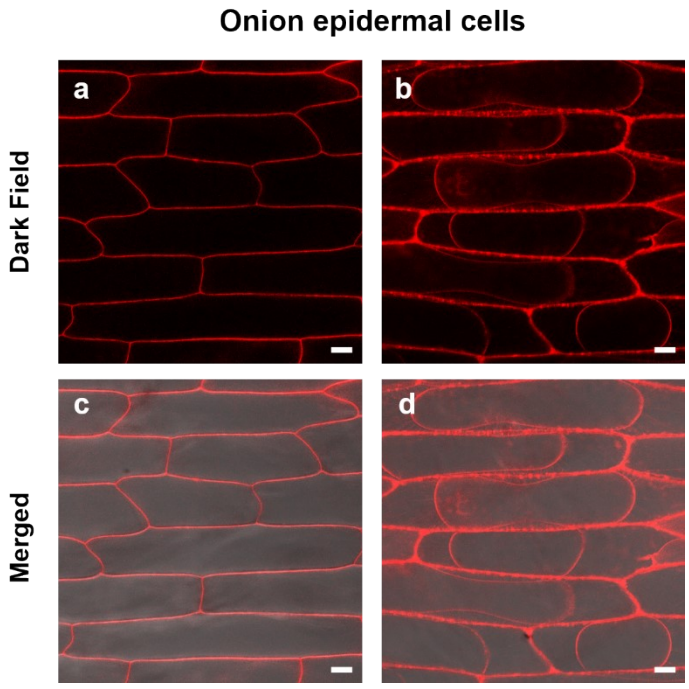

Figure S11. Laser scanning confocal microscopy images in onion epidermal cells, which were first stained with APMem-1 (10.0 μM) for 5 min and then incubated in 0.3 g/mL sucrose solution for different times to achieve plasmolysis: (a, c) 0 min; (b, d) 20 min. Scale bar = 50 μm.

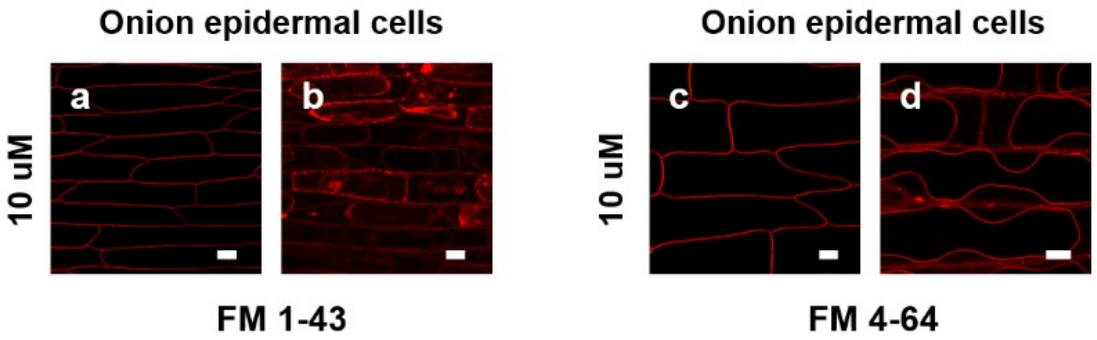

Figure S12. Laser scanning confocal microscopy images in onion epidermal cells, which were first stained with FM 1-43 and FM 4-64 (10.0 μM) for 5 min and then incubated in 0.3 g/mL sucrose solution for different times to achieve plasmolysis: (a, b) FM 1-43, Scale bar = 50 μm, 20 μm; (c, d) FM 4-64, Scale bar = 50 μm, 50 μm.

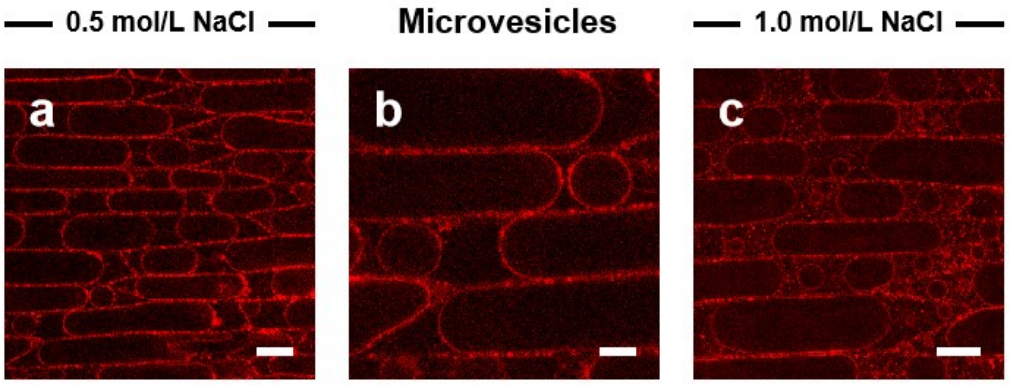

Figure S13. Laser scanning confocal microscopy images in onion epidermal cells, which were first stained with APMem-1 (10.0 μM) for 5 min and then incubated in sodium chloride solution for different concentration to achieve plasmolysis with 30min: (a) 0.5 mol/L NaCl, Scale bar = 50 μm; (b) The neonatal microvesicles in the process, Scale bar = 20 μm; (c) 1.0 mol/L NaCl, Scale bar = 50 μm.

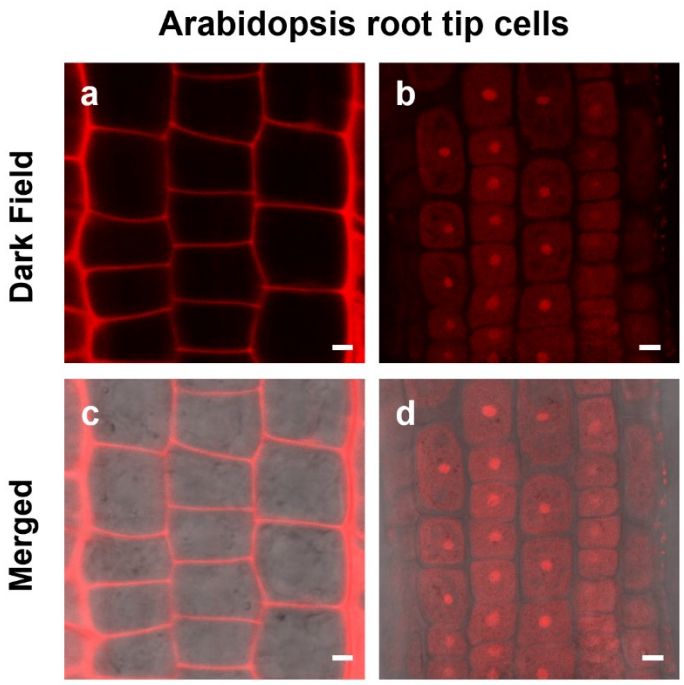

Figure S14. Comparison of laser scanning confocal microscopy images of stained seedling roots of *Arabidopsis thaliana* (APMem-1, 10.0 μM, 5 min) treated with DMSO (b, d) and without DMSO (a, c). (a, c) Scale bar = 5 μm, (b, d) Scale bar = 10 μm.

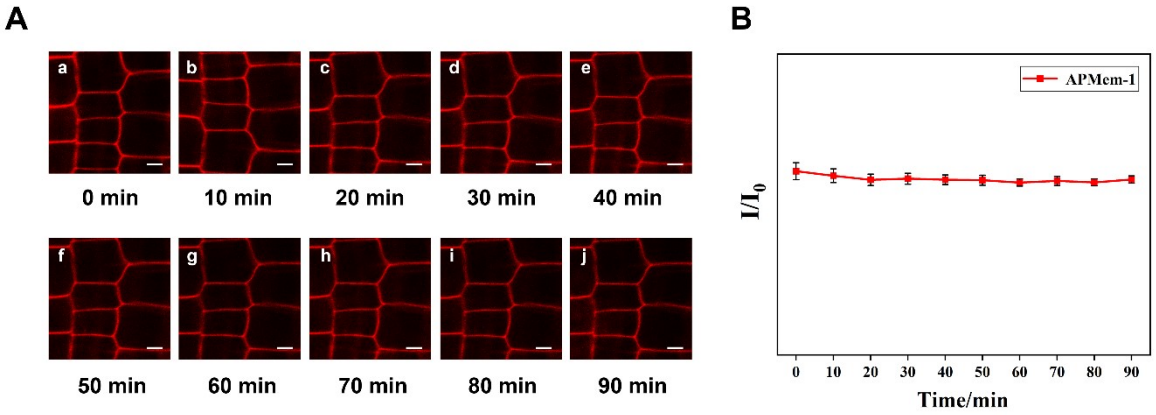

Figure S15. (A) The changes of laser scanning confocal microscopy images in seedling roots of *Arabidopsis thaliana* stained with APMem-1 (10.0 μM) for 5 min versus irradiation time at 561 nm using the excitation source of the used microscope: (a) APMem-1 (0 min); (b) APMem-1 (10 min); (c) APMem-1 (20 min); (d) APMem-1 (30 min); (e) APMem-1 (40 min); (f) APMem-1 (50 min); (g) APMem-1 (60 min); (h) APMem-1 (70 min); (i) APMem-1 (80 min); (j) APMem-1 (90 min). Scale bar = 10 μm. (B) The change of PL intensity of APMem-1 inserted inside the cell membranes versus irradiation time at 561 nm using the excitation source of the used microscope.

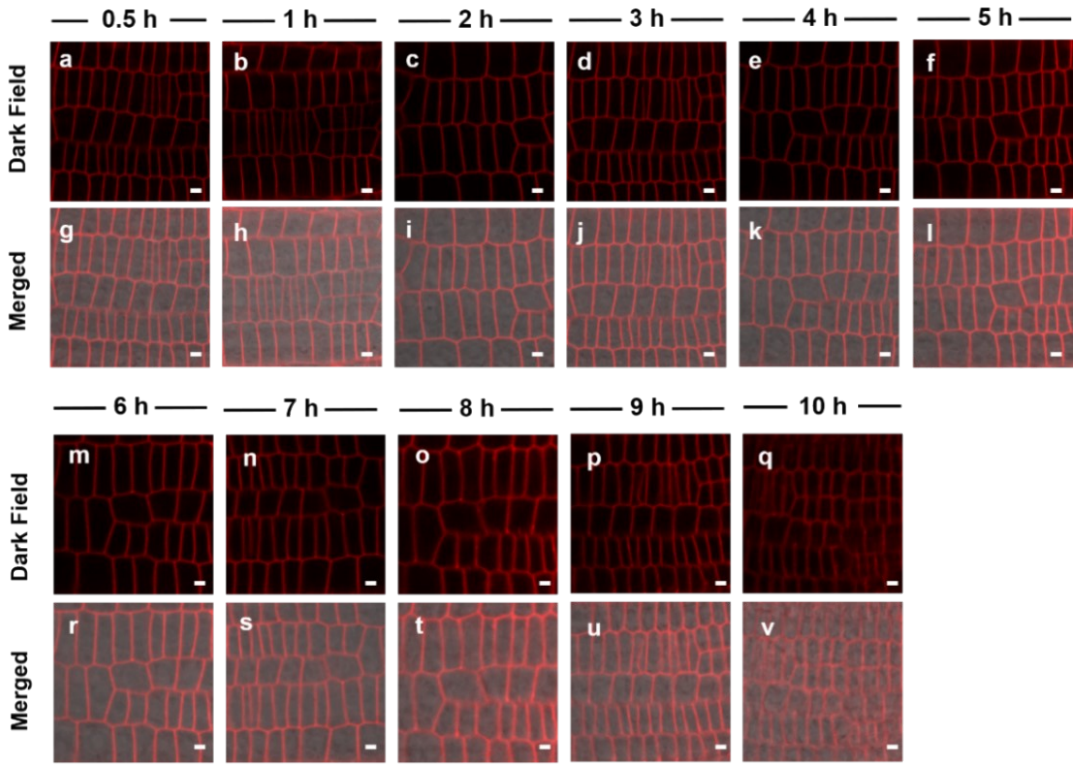

Figure S16. Laser scanning confocal microscopy images in seedling roots of *Arabidopsis thaliana* stained with APMem-1 (10.0 μM probes incubated for 5 min) at various time points: (a, g) APMem-1 (0.5 h); (b, h) APMem-1 (1 h); (c, i) APMem-1 (2 h); (d, j) APMem-1 (3 h); (e, k) APMem-1 (4 h); (f, l) APMem-1 (5 h); (m, r) APMem-1 (6 h); (n, s) APMem-1 (7 h); (o, t) APMem-1 (8 h); (p, u) APMem-1 (9 h); (q, v) APMem-1 (10 h). Scale bar = 10 μm.

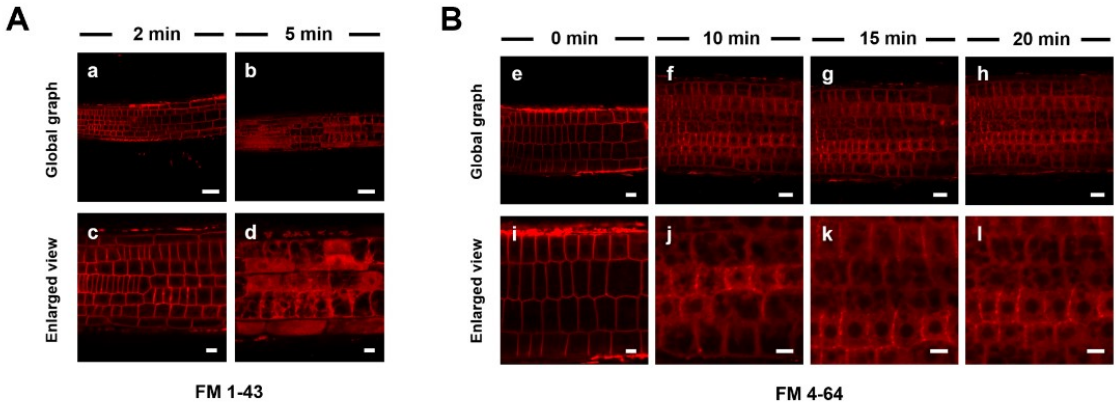

Figure S17. Laser scanning confocal microscopy images of seedling roots of Arabidopsis thaliana stained with (A) FM 1-43 (B) FM 4-64 (10.0 μM probes incubated for 5 min) at various time points. (a, b, e, f, g, h) Scale bar= 20 μm; (c, d, i, j, k, l) Scale bar= 10 μm.

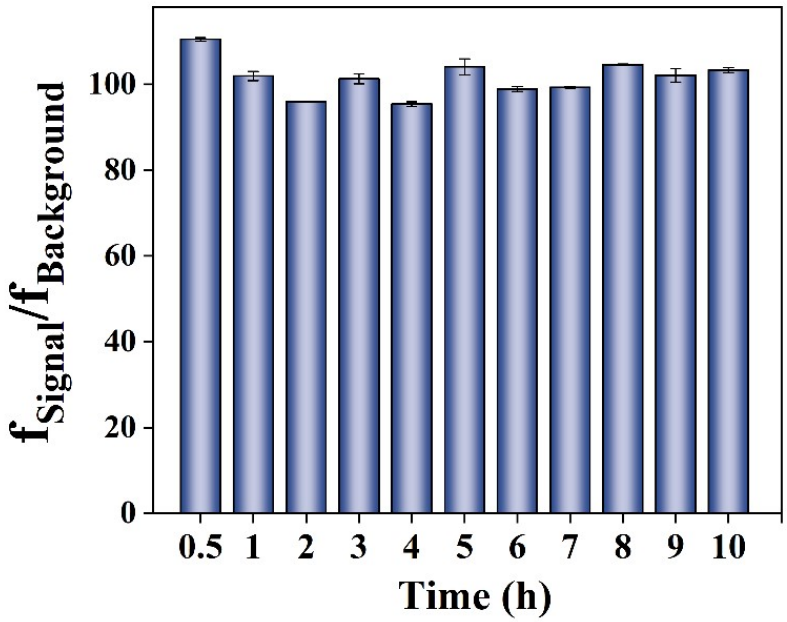

Figure S18. The values of f_{Signal} /$f_{Background}$ during 1 – 10 h imaging time.

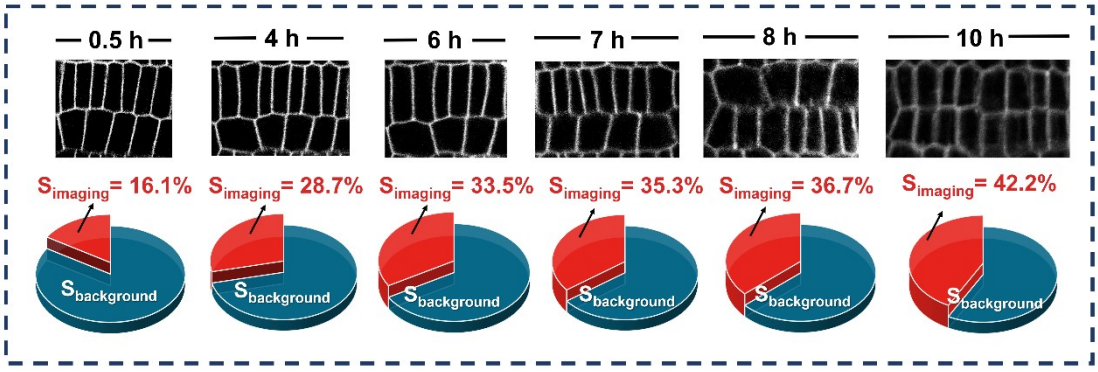

Figure S19. High-resolution image analyses of imaging performance for seedling roots of *Arabidopsis thaliana* stained with APMem-1 in imaging completeness and imaging specificity. $S_{imaging}$ and $S_{Background}$ represent the ratios of signal area and background area to the whole area.

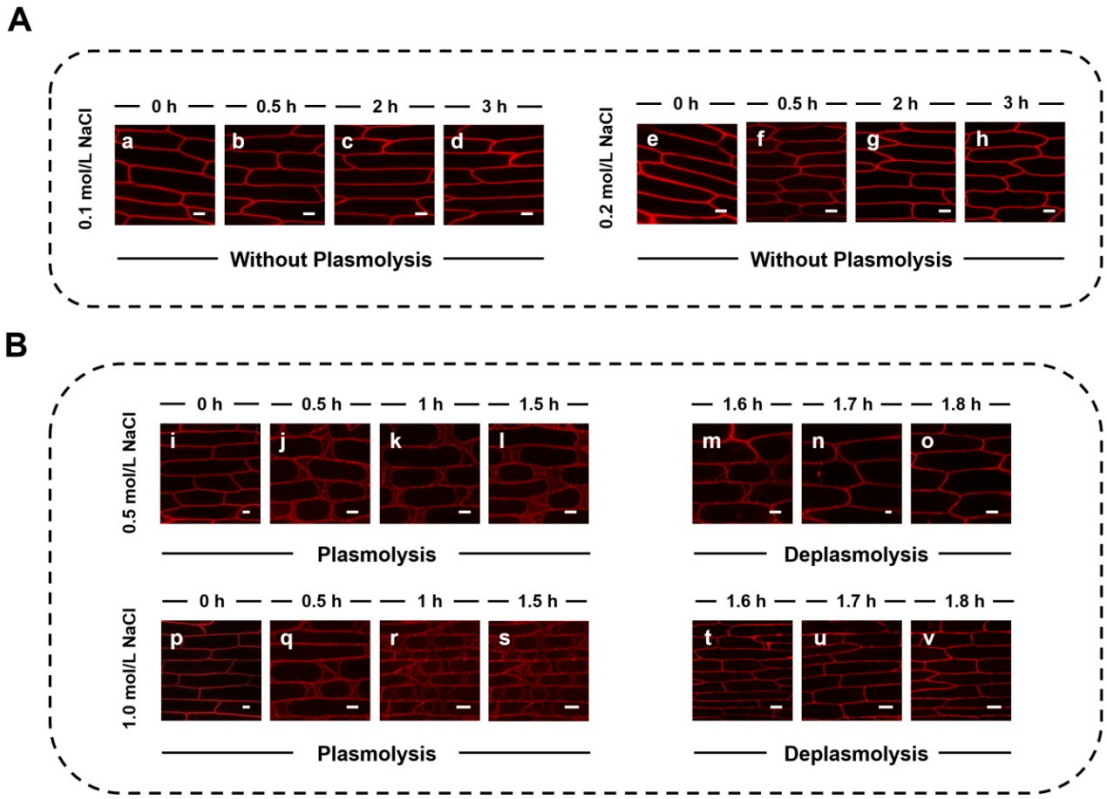

Figure S20. Laser scanning confocal microscopy images in onion epidermal cells, which were first stained with APMem-1 (10.0 μM) for 5 min and then incubated with different concentrations of NaCl solution at various time points (A) 0.1 mol/L NaCl, Scale bar = 50 μm; 0.2 mol/L NaCl, Scale bar = 50 μm; (B) 0.5 mol/L NaCl, Scale bar = 50 μm (n: 20 μm); 1.0 mol/L NaCl; Scale bar = 50 μm.

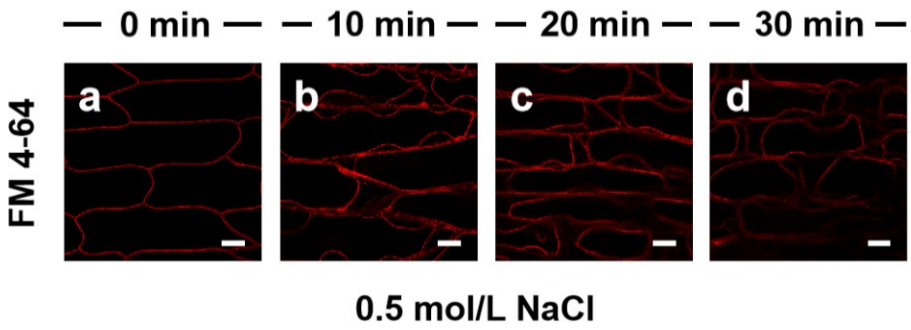

Figure S21. Laser scanning confocal microscopy images in onion epidermal cells, which were first stained with FM 4-64 (10.0 μM) for 5 min and then incubated in 0.5mol/L NaCl solution at various time points to achieve plasmolysis; Scale bar = 50 μm.

4. Spectra of Compounds

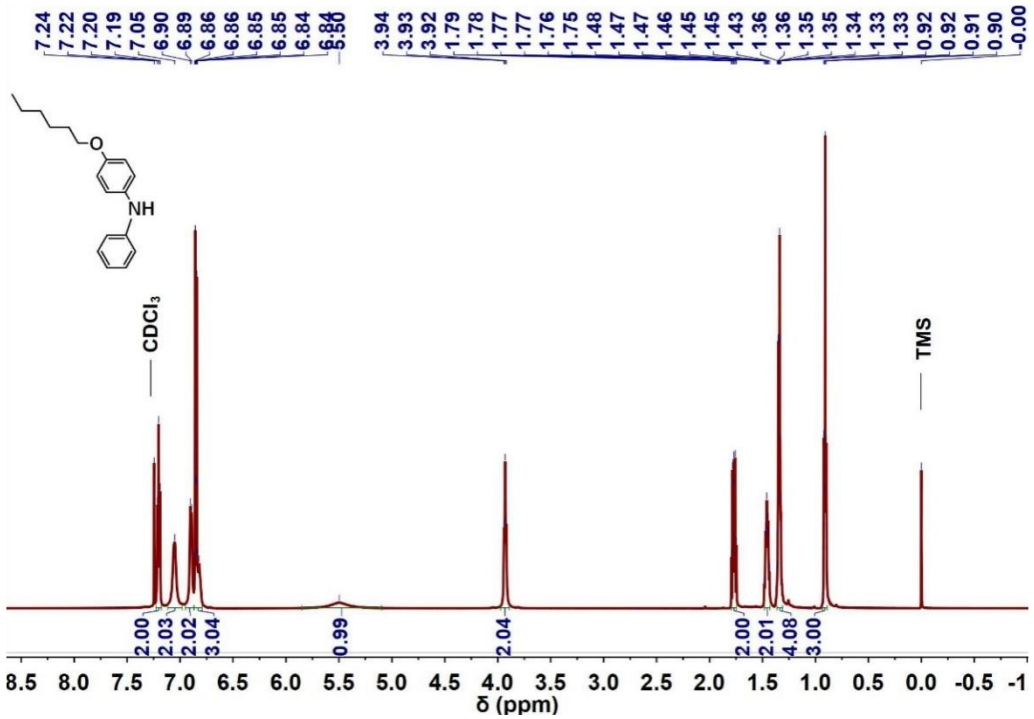

Figure S22 ^{1}H NMR spectra of 4-(hexyloxy)-N-phenylaniline in $CDCl_3$

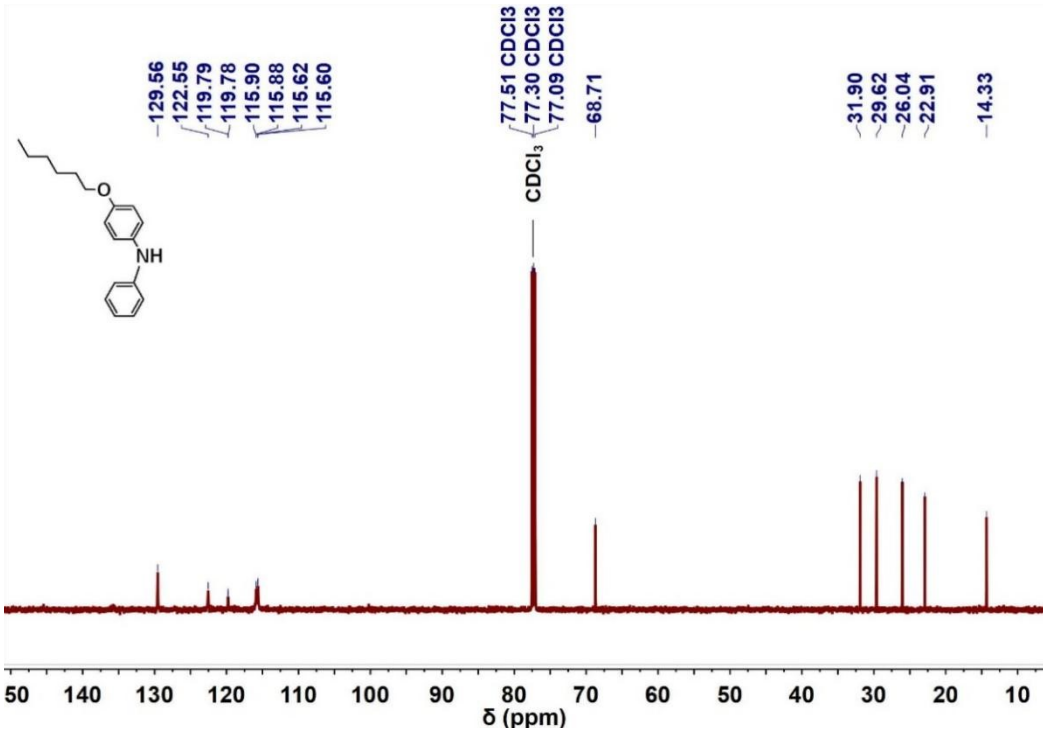

Figure S23 ^{13}C NMR spectra of 4-(hexyloxy)-N-phenylaniline in $CDCl_3$

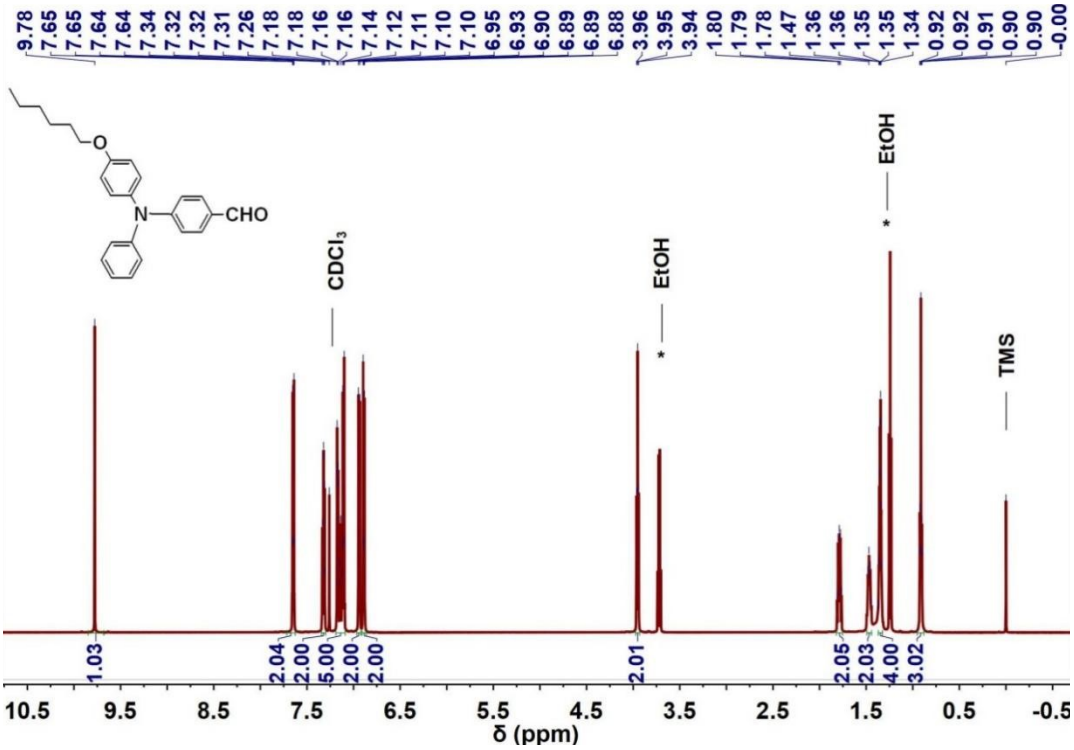

Figure S24 ^{1}H NMR spectra of 4-((4-(hexyloxy)phenyl)(phenyl)amino)benzaldehyde in $CDCl_3$

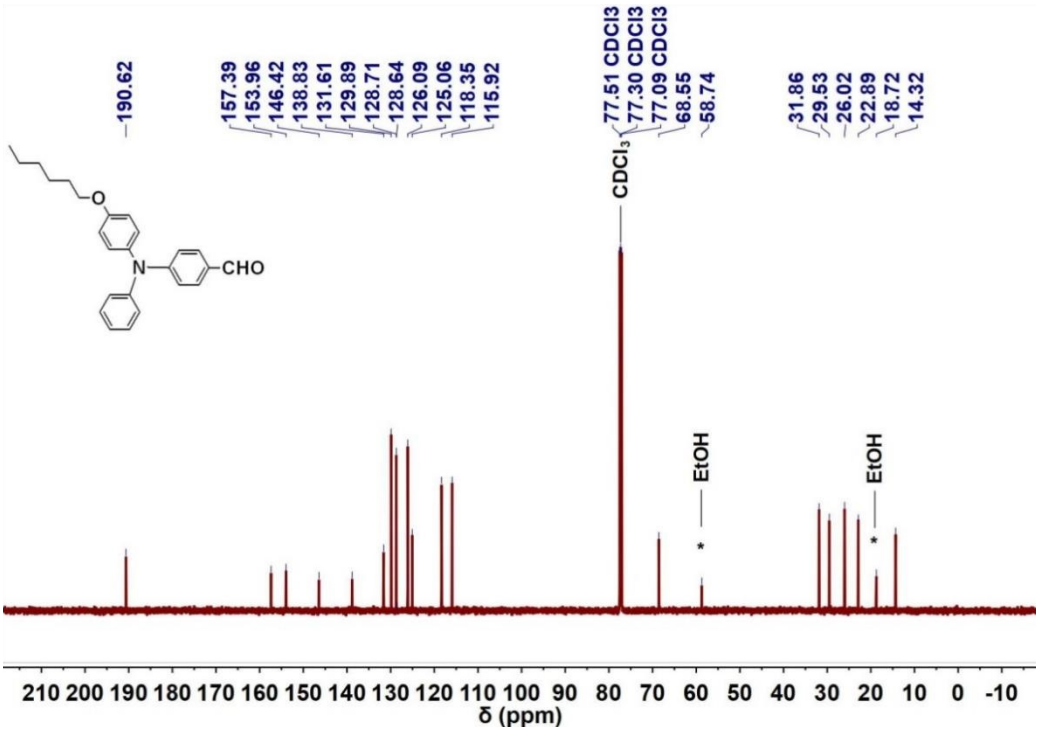

Figure S25 ^{13}C NMR spectra of 4-((4-(hexyloxy)phenyl)(phenyl)amino)benzaldehyde in $CDCl_3$

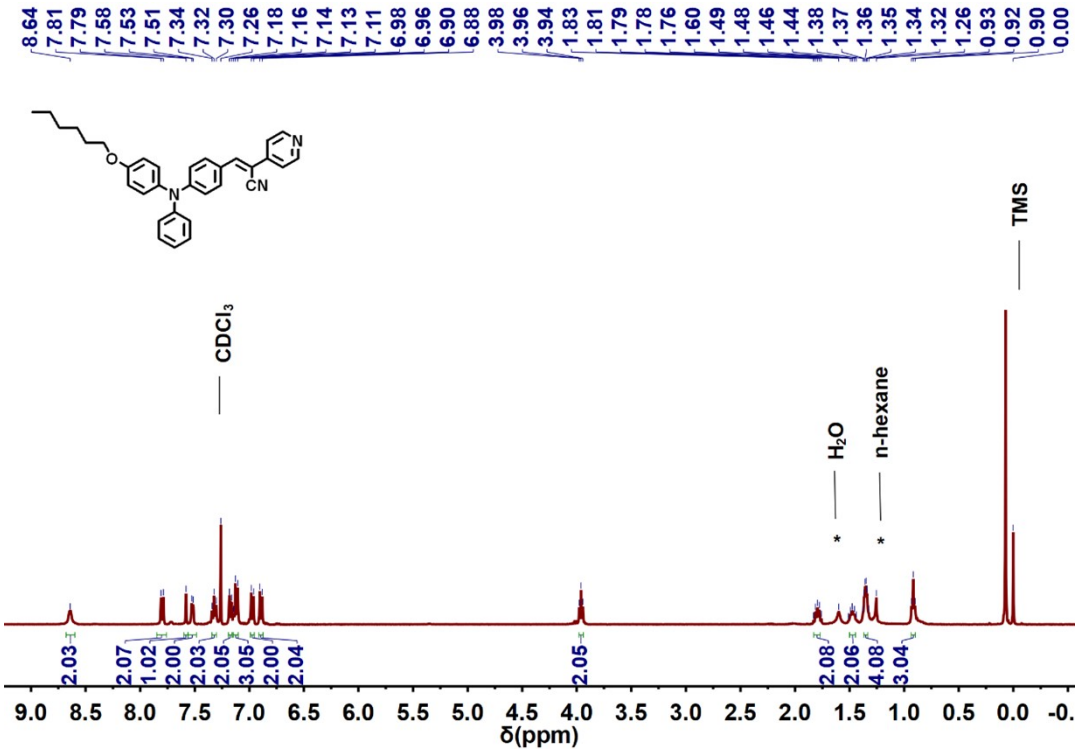

Figure S26 ^{1}H NMR spectra of 3-(4-((4-(hexyloxy)phenyl)(phenyl)amino)phenyl)-2-(pyridin-4-yl)acrylonitrile in $CDCl_3$

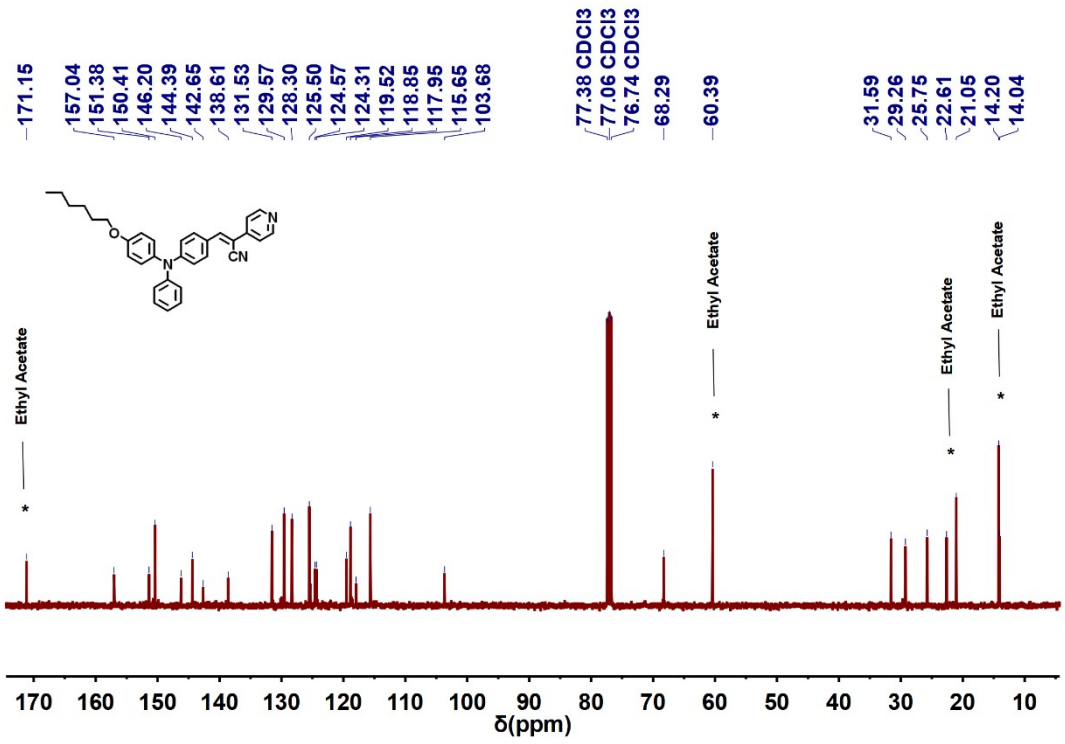

Figure S27 ^{13}C NMR spectra of 3-(4-((4-(hexyloxy)phenyl)(phenyl)amino)phenyl)-2-(pyridin-4-yl)acrylonitrile in $CDCl_3$

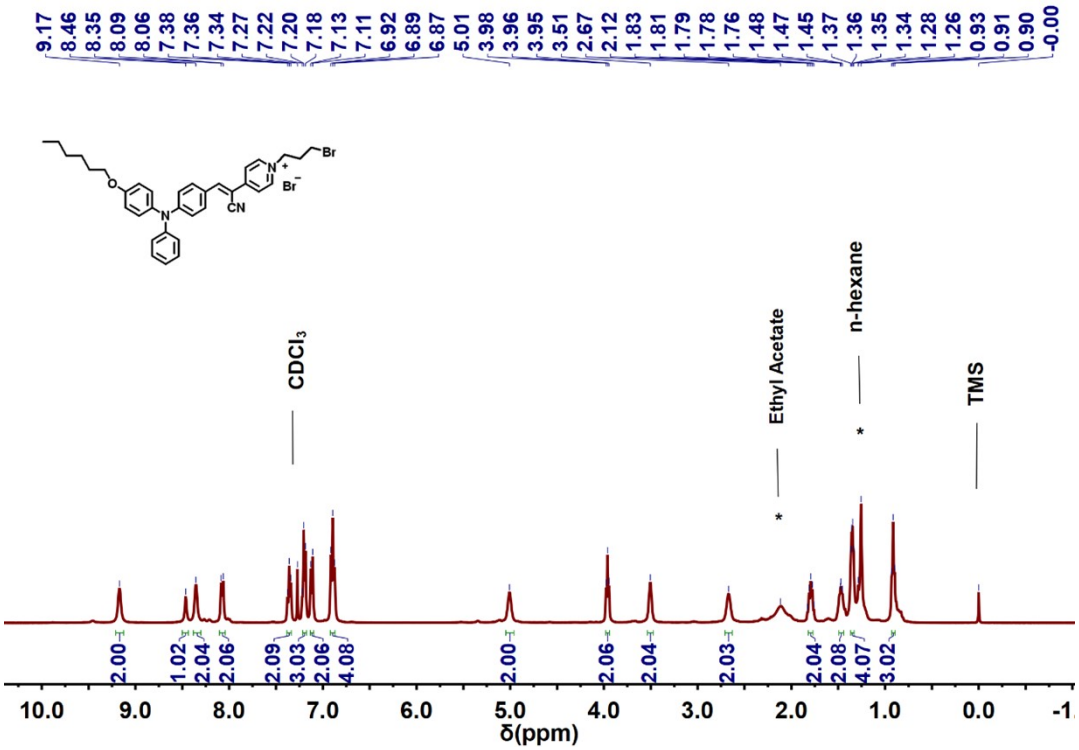

Figure S28 ^{1}H NMR spectra of 1-(3-bromopropyl)-4-(1-cyano-2-(4-((4-(hexyloxy)phenyl)(phenyl)amino)phenyl)vinyl)pyridin-1-ium in $CDCl_3$

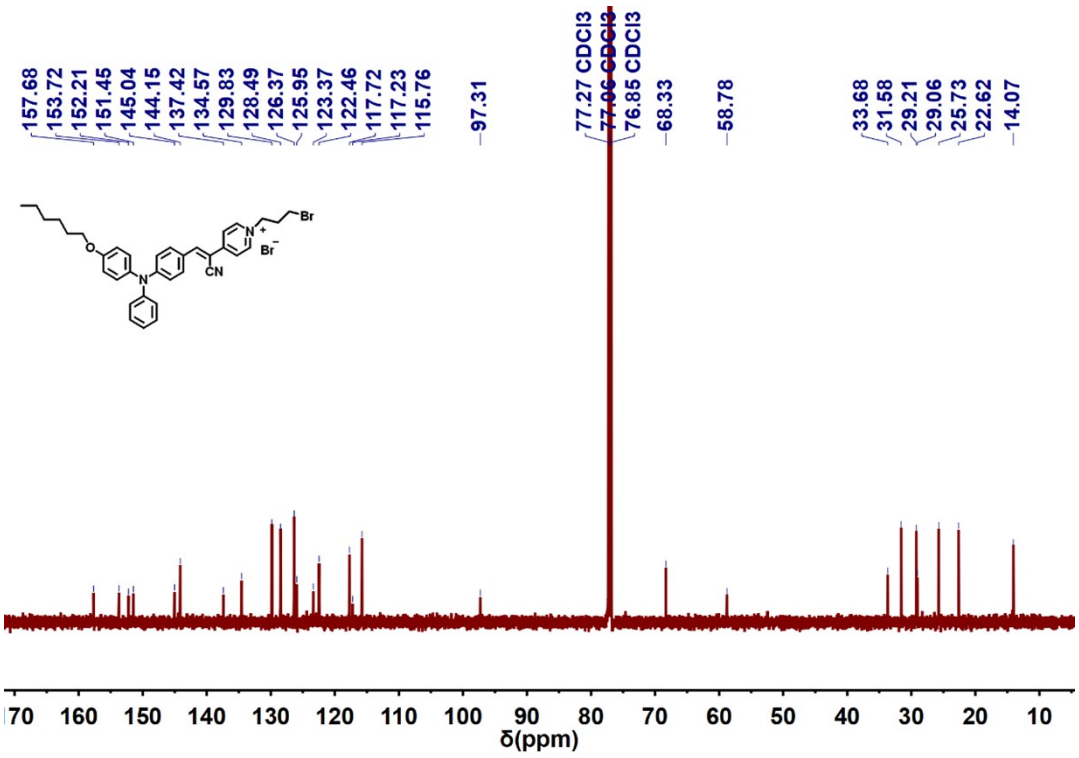

Figure S29 ^{13}C NMR spectra of 1-(3-bromopropyl)-4-(1-cyano-2-(4-((4-(hexyloxy)phenyl)(phenyl)amino)phenyl)vinyl)pyridin-1-ium in $CDCl_3$

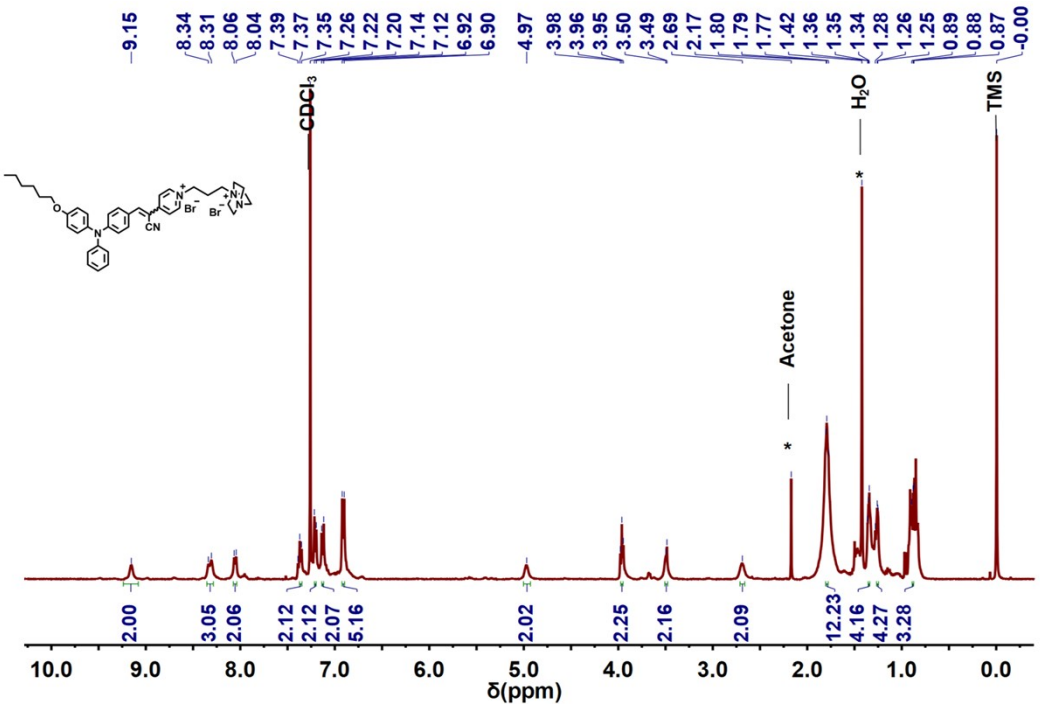

Figure S30 ^{1}H NMR spectra of (Z)-1-(3-(4-(1-cyano-2-(4-((4-(hexyloxy)phenyl)(phenyl)amino)phenyl)vinyl)pyridin-1-ium-1-yl)propyl)-1,4-diazabicyclo[2.2.2]octan-1-ium in $CDCl_3$

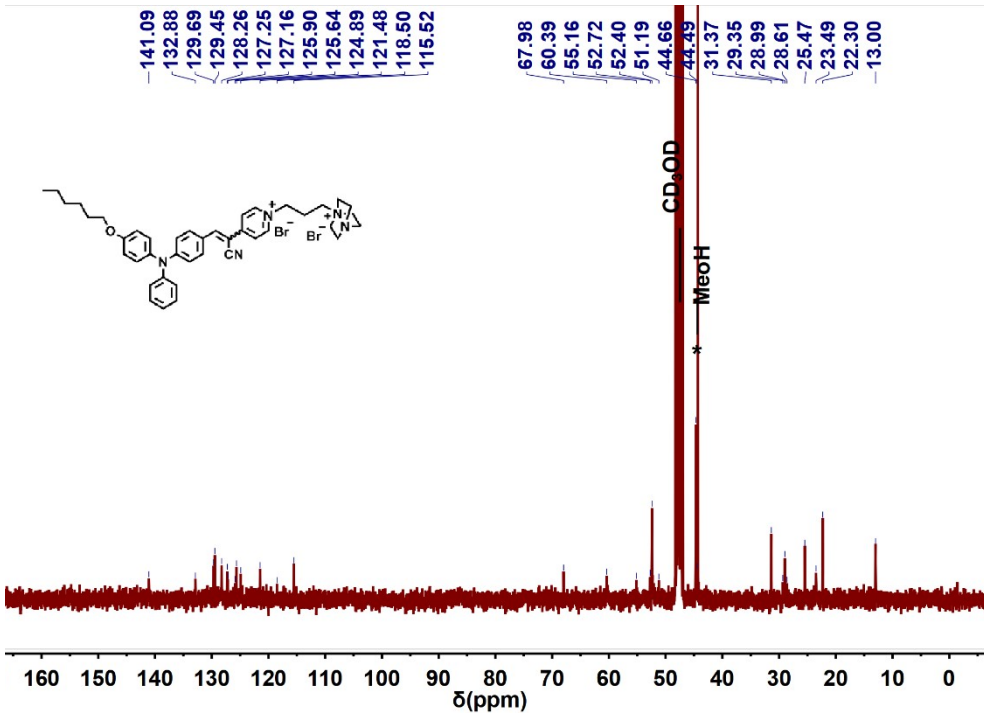

Figure S31 ^{13}C NMR spectra of spectra of (Z)-1-(3-(4-(1-cyano-2-(4-((4-(hexyloxy)phenyl)(phenyl)amino)phenyl)vinyl)pyridin-1-ium-1-yl)propyl)-1,4-diazabicyclo[2.2.2]octan-1-ium in CD_3OD

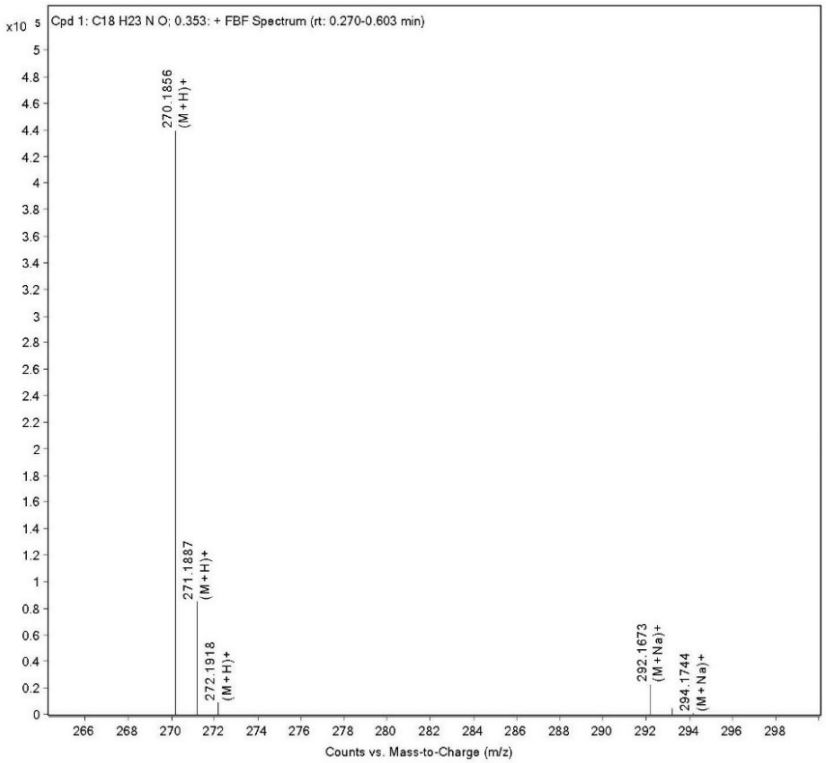

Figure S32 High-resolution mass spectrum of 4-(hexyloxy)-N-phenylaniline

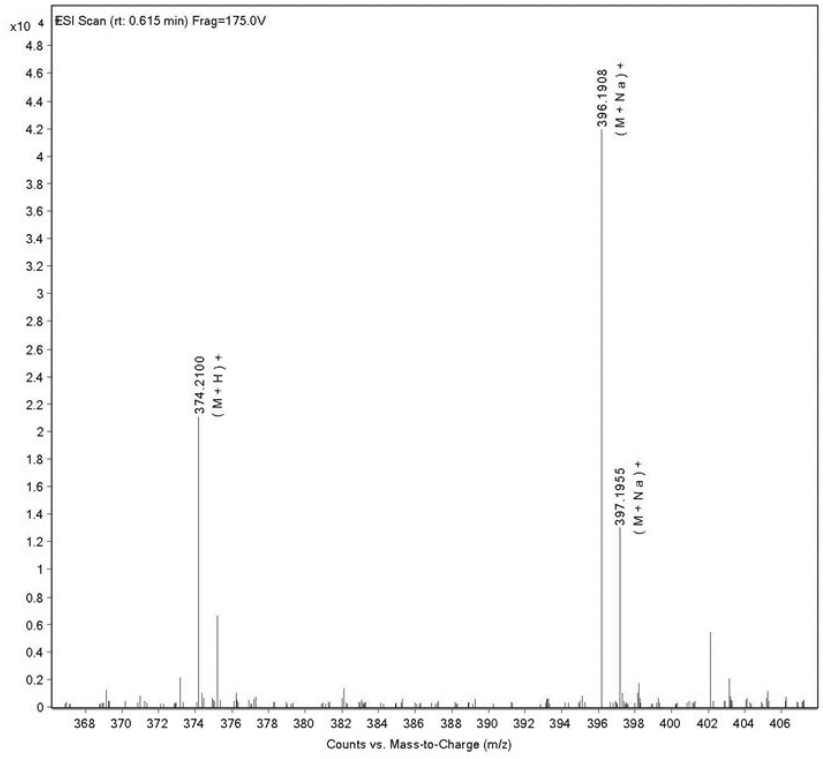

Figure S33 High-resolution mass spectrum of 4-((4-(hexyloxy)phenyl)(phenyl)amino) benzaldehyde

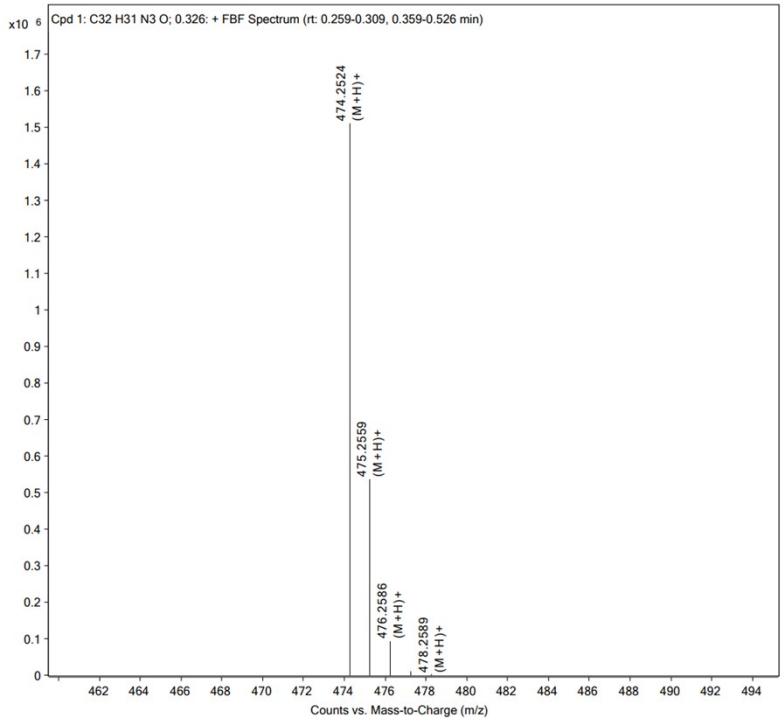

Figure S34 High-resolution mass spectrum of (Z)-3-(4-((4-(hexyloxy)phenyl)(phenyl)methyl)phenyl)-2-(pyridin-4-yl)acrylonitrile

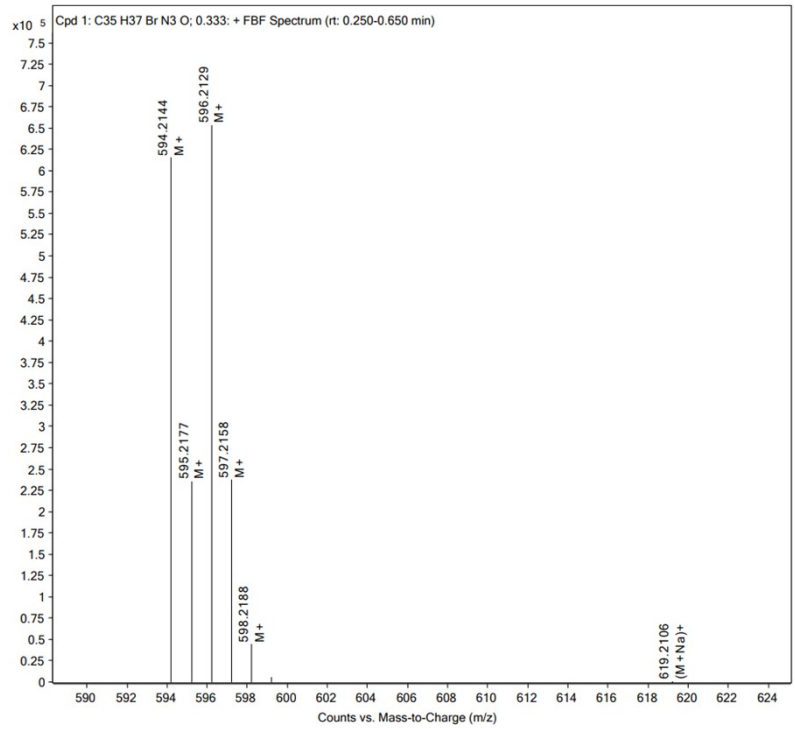

Figure S35 High-resolution mass spectrum of (Z)-1-(3-bromopropyl)-4-(1-cyano-2-(4-((4-(hexyloxy)phenyl)(phenyl)amino)phenyl)vinyl)pyridin-1-ium.

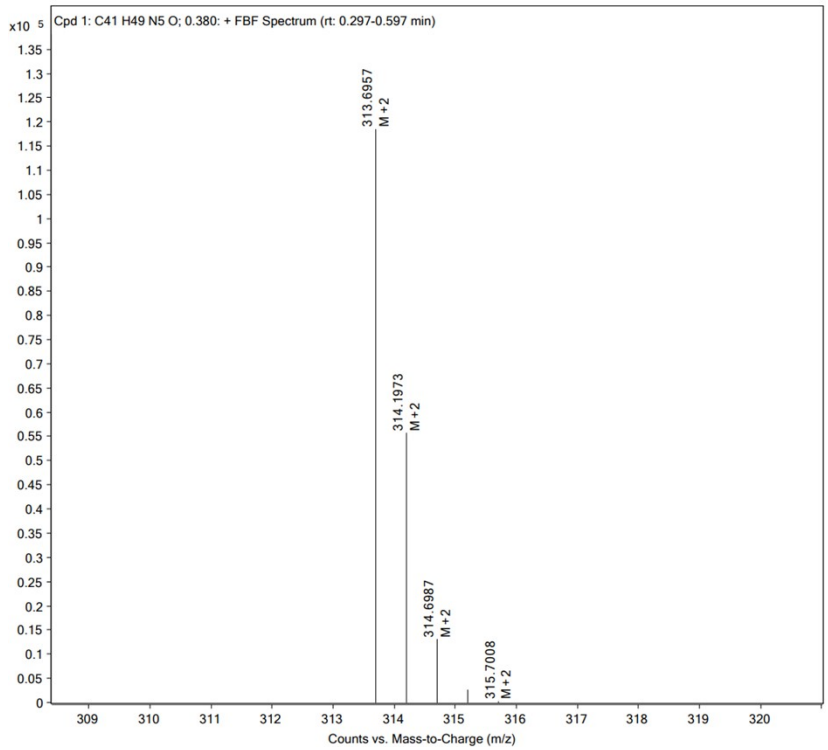

Figure S36 High-resolution mass spectrum of APMem-1